Physics of the Earth and Planetary Interiors 172 (2009) 157–168

Contents lists available at ScienceDirect

Physics of the Earth and Planetary Interiors

journal homepage: www.elsevier.com/locate/pepi

Rock magnetic properties and relative paleointensity stack between 13 and 24 kyr BP calibrated ages from sediment cores, Lake Moreno (Patagonia, Argentina)

María A. Irurzun[a,b], Claudia S.G. Gogorza[a,b,*], Sebastián Torcida[c], Juan M. Lirio[d], Héctor Nuñez[d], Paula G. Bercoff[b,e], Marcos A.E. Chaparro[a,b], Ana M. Sinito[a,b]

[a] Instituto de Física Arroyo Seco, Universidad Nacional del Centro de la Provincia de Buenos Aires, Pinto 399, 7000 Tandil, Argentina
[b] Consejo Nacional de Investigaciones Científicas y Técnicas, Rivadavia 1917, C1033AAJ Buenos Aires, Argentina
[c] Instituto Multidisciplinario de Ecosistemas y Desarrollo Sustentable, Universidad Nacional del Centro de la Provincia de Buenos Aires, Pinto 399, 7000 Tandil, Argentina
[d] Instituto Antártico Argentino, Cerrito 1248, Buenos Aires, Argentina
[e] Facultad de Matemática, Astronomía y Física, Universidad Nacional de Córdoba, Ob. Trejo 242, Córdoba, Argentina

ARTICLE INFO

Article history:
Received 25 March 2008
Received in revised form 13 August 2008
Accepted 19 August 2008

Keywords:
Relative paleointensity
Sediment cores
South America
Lake Moreno
Pseudo-Thellier

ABSTRACT

We conducted a detailed study of natural remanence and rock magnetic properties on three sediment cores from Lake Moreno (Patagonia, Argentina). Based on these measurements, we constructed a relative paleointensity stack for the period 13–24 kyr BP calibrated ages. Rock magnetic properties of the sediment cores showed uniform magnetic mineralogy and grain size, suggesting that they were suitable for relative paleointensity studies. The remanent magnetisation at 20 mT ($NRM_{20\,mT}$) was normalised using the anhysteretic remanent magnetisation at 20 mT ($ARM_{20\,mT}$), the saturation of the isothermal remanent magnetisation at 20 mT ($SIRM_{20\,mT}$) and the low-field magnetic susceptibility (k). Spectral analysis showed that the normalised records were not affected by local environmental conditions. The recorded pseudo-Thellier paleointensity was compared with records obtained from conventional normalising methods. Comparing the paleointensity curves with others obtained previously in other lakes in the area has allowed us to reach reliable conclusions about centennial-scale features.

1. Introduction

Studies of lacustrine sequences have provided fundamental information about relative paleointensity (RPI) variations of the geomagnetic field. However, several tests for sedimentary paleointensity based on rock magnetic criteria (Banerjee et al., 1981; Tauxe, 1993) must be performed to establish reliability of the data. King et al. (1983) proposed the concept of "magnetic uniformity", i.e. the absence of changes in relative grain sizes and concentrations. In order to minimize the effects of down-core variability, the natural remanent magnetisation (NRM) is normalised by some magnetic parameter. Different normalisers have been discussed (Tauxe, 1993), including anhysteretic remanent magnetisation (ARM), saturation isothermal remanent magnetisation (SIRM) and magnetic susceptibility (k), and numerous studies have been published (Brachfeld and Banerjee, 2000; Gogorza et al., 2004, 2006; Peck et al., 1996; Sagnotti et al., 2001; St-Onge et al., 2003; Blanchet et al., 2006; Macri et al., 2006; Richter et al., 2006; Hofmann and Fabian, 2007). In order to test the reliability of the RPI data, the coherence function (Tauxe and Wu, 1990) between the normalised remanence and the respective normaliser is calculated. This quantitatively estimates the degree to which the normalised intensity records are biased by environmental variations in grain size and concentration.

Several authors argue that the appropriate demagnetisation of the NRM is the only important factor for constructing a reliable paleointensity from sediments (Levi and Banerjee, 1976; Valet and Meynadier, 1998). Tauxe et al. (1995) proposed the pseudo-Thellier method to determine if the records could be affected by unremoved viscosity, which relies on comparing the NRM lost during demagnetisation and the ARM gained within the same range of coercivities. It has been argued that this method diminishes the environmental contamination of the paleointensity signal better than conventional normalising methods (Kruiver et al., 1999). In this paper, we compare the paleointensity obtained by the standard normalising method and the results obtained from one core with the pseudo-Thellier method. In addition, we perform rock magnetic analyses to study possible environmental influences on the sediment in the studied cores.

Improved knowledge about relative variations of the geomagnetic field over the last few hundred thousand years has allowed the construction of global reference paleointensity curves, which are

* Corresponding author at: Instituto de Física Arroyo Seco, Universidad Nacional del Centro de la Provincia de Buenos Aires, Pinto 399, 7000 Tandil, Argentina. Tel.: +54 2293 439660; fax: +54 2293 439669.
E-mail address: cgogorza@exa.unicen.edu.ar (C.S.G. Gogorza).

0031-9201/$ – see front matter © 2008 Elsevier B.V. All rights reserved.
doi:10.1016/j.pepi.2008.08.018

useful for defining high-resolution age models in appropriate sedimentary sequences (Sagnotti et al., 2001; Guyodo and Valet, 1996). The research presented in this paper helps mitigate the extremely uneven global distribution of data.

Previous studies have been carried out at the local scale (Gogorza et al., 2004, 2006), and were successfully compared with records from other sites in the world (Brachfeld and Banerjee, 2000; Brachfeld et al., 2003; Constable, 1985; Peck et al., 1996; St-Onge et al., 2003). Some discrepancies were observed between previously reported results in the period 14–23 kyr BP calibrated ages. This study aims to determine whether these differences came from an incorrect time correlation or from different rock magnetic characteristics, and to refine our understanding of the temporal geomagnetic field intensity during this period.

2. Sedimentology

Lake Moreno is a closed basin of about 120,000 m^2, located on the eastern side of the Andean Patagónica Cordillera, at about 41°S 71°30′W (Fig. 1) and approximately 17 km northwest of San Carlos de Bariloche, Argentina. A land barrier divides the lake into two: west Moreno and east Moreno, respectively. The average annual temperature is about 8.7 °C and the annual precipitation is between 150 and 180 cm/yr. This region presents one of the most marked humidity gradients of the world, clearly reflected by vegetation: from west to east, the moist forest is replaced by the Patagonian steppe in less than 50 km (Bianchi et al., 1999). It is related to series of large glacially carved lakes. The basement rocks of the basin crop out in the lake catchment area and show evidence of glaciation striation and some erratic blocks of different composition. The more ancient lacustrine sediments are on the top of these rocks; the sedimentary sequence consists of reddish clays thin layered with little clastic rocks (dropstones), especially at the bottom. These evidences indicate a glacial origin of the Lake Moreno and a glaciolacustrine origin of the reddish clays; the youngest sedimentary column is not present, due to the erosion. The present vegetation covers most of the glaciolacustrine sequence that lies over the lake coast. A more detailed description of the sedimentology of Lake Moreno is given in Gogorza et al. (2006).

Three principal lithologies are present in the sediment column of the lake, and are, from bottom to top: light reddish clayey silt (lithology A), light grey greenish clay (lithology B) and light grey clay (lithology C). Good correlation between the cores was established based on 28 tephra layers located mostly in the upper part and specific susceptibility records.

Two different facies can be recognized: a basal glaciolacustrine facies (which includes lithologies A and B and tephra layers) named the "Lake Elpalafquen" facies, and a younger lacustrine facies (lithology C and tephra layers) or the "Lake Moreno" facies (Gogorza et al., 2006). The "Lake Elpalafquen" facies has been recognized in cores from other lakes of the area (El Trébol, Escondido and Mascardi), and outcrops at the Lake Nahuel Huapi coast (del Valle et al., 2000). These sediments represent sedimentation during Late Pleistocene times, when a large pro-glacial lake, Lake Elpalafquen (del Valle et al., 2000), existed in the region. On the other hand, the "Lake Moreno" facies represents lacustrine sedimentation with no direct glacial influence. These were deposited mainly during Holocene time, after the collapse of Lake Elpalafquen, which gave rise to the formation of the present lakes of the region.

3. Materials and methods

The three cores investigated in this study are labelled lmor-1, lmor98-1 and lmor98-2 (Fig. 1); they were collected with a push corer from the shoreline (a marshy site approximately 1 m above the present Lake Moreno level); the length of the cores varies from 2.5 to 4 m. Individual samples were taken by inserting an 8 cm^3 cubic plastic box into the surface; 371 samples were collected.

The magnetic susceptibility at low frequency (specific, X_{lf}, and volumetric, k) was measured with the Bartington Instruments MS2 system. A Pulse Magnetizer model IM-10-30 ASC Scientific and a Shielded Demagnetiser Molspin Ltd. with an ARM device were used for IRM and ARM acquisition experiments. Remanence measurements for all samples were performed with a Spinner Fluxgate Magnetometer Minispin, Molspin Ltd.

NRM was systematically demagnetised by alternating field (AF) at 0, 5, 10, 15, 20, 25, 30, 35, 40, 45, 50, 60, 70, 80 and 95 mT. The median destructive field (MDF_{NRM}) was also determined. ARM was acquired in a peak alternating field of 95 mT with a steady bias field of 0.1 mT ($ARM_{95\,mT}$) and was subsequently demagnetised to a peak AF of 95 mT using the same field steps as for NRM demagnetisation. IRM was acquired at room temperature in increasing steps up to 1.2 T reaching saturation (SIRM); subsequently, AF demagnetisation of IRM was measured using the same steps as for NRM demagnetisation. After that, a 1.2 T field was imparted at room temperature and progressive demagnetisation was applied up to 1.2 T for the DC experiment.

Sub-samples were taken from core lmor-1 for hysteresis measurements and thermal demagnetisation. The hysteresis parameters were obtained using a VSM Lake Shore 7300 with a maximum applied field of 1.5 T; we then calculated the magneto-granulometric indicative ratios of saturation remanence to saturation magnetisation (M_{RS}/M_S) and coercivity of remanence to coercive force (H_{CR}/H_C).

Thermal demagnetisation studies were carried out using a thermal specimen demagnetiser, model TD-48 ASC Scientific. Before

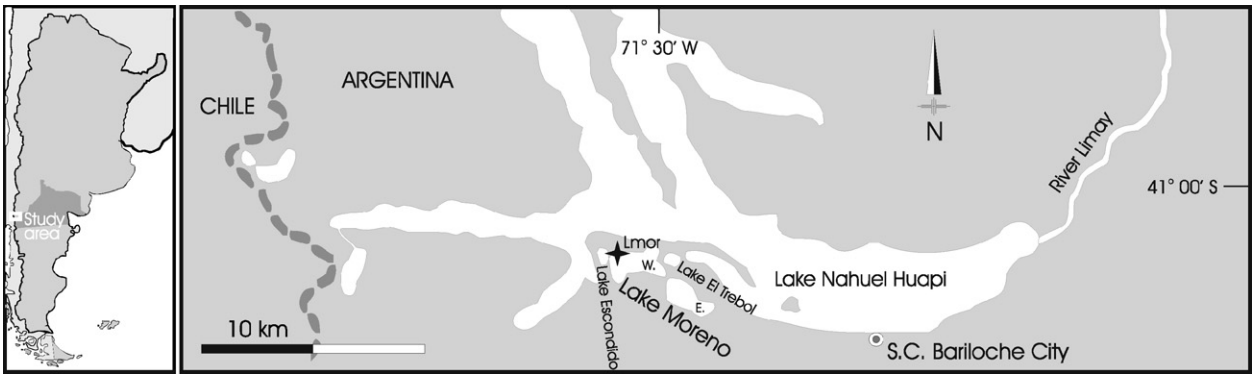

Fig. 1. Geographical location of Lake Moreno: W: west Moreno; E: east Moreno; ✦ Lmor: coring sites.

thermal experiments, samples were magnetised, acquiring a SIRM. They were then heated in increasing stepwise temperatures in air, from room temperature (RT) to 700 °C. After each step, remanent magnetisation (RM) and k were measured for cooled samples. Stepwise thermal demagnetisation curves and magnetic susceptibility measurements were determined and unblocking temperatures (T_U) were estimated.

The depth scales of all the cores were adjusted to the depth scale of a master core (lmor-1) using some visually distinct lithostratigraphic horizons and X_{lf} tie lines for correlation (Irurzun et al., 2008). As tephra layers represent rapid instantaneous deposition of thick layers, while the rest of the sediments represent slow accumulation, and because tephra is not a very good magnetic recorder, tephra layers were removed from the sequence and the resulting gaps were closed, creating a "shortened depth" scale (Gogorza et al., 1999).

The individual RPI records obtained by normalising methods were stacked using the arithmetic mean over the time interval 13–24 kyr BP calibrated ages and a RPI record for core lmor-1 was also obtained by pseudo-Thellier method (Tauxe et al., 1995).

4. Sediment-magnetic characterization

Fig. 2 shows the lithology, X_{lf}, NRM intensity and MDF_{NRM} logs for master core lmor-1. The NRM intensity shows variations similar to those in the concentration-dependent parameter X_{lf}, which

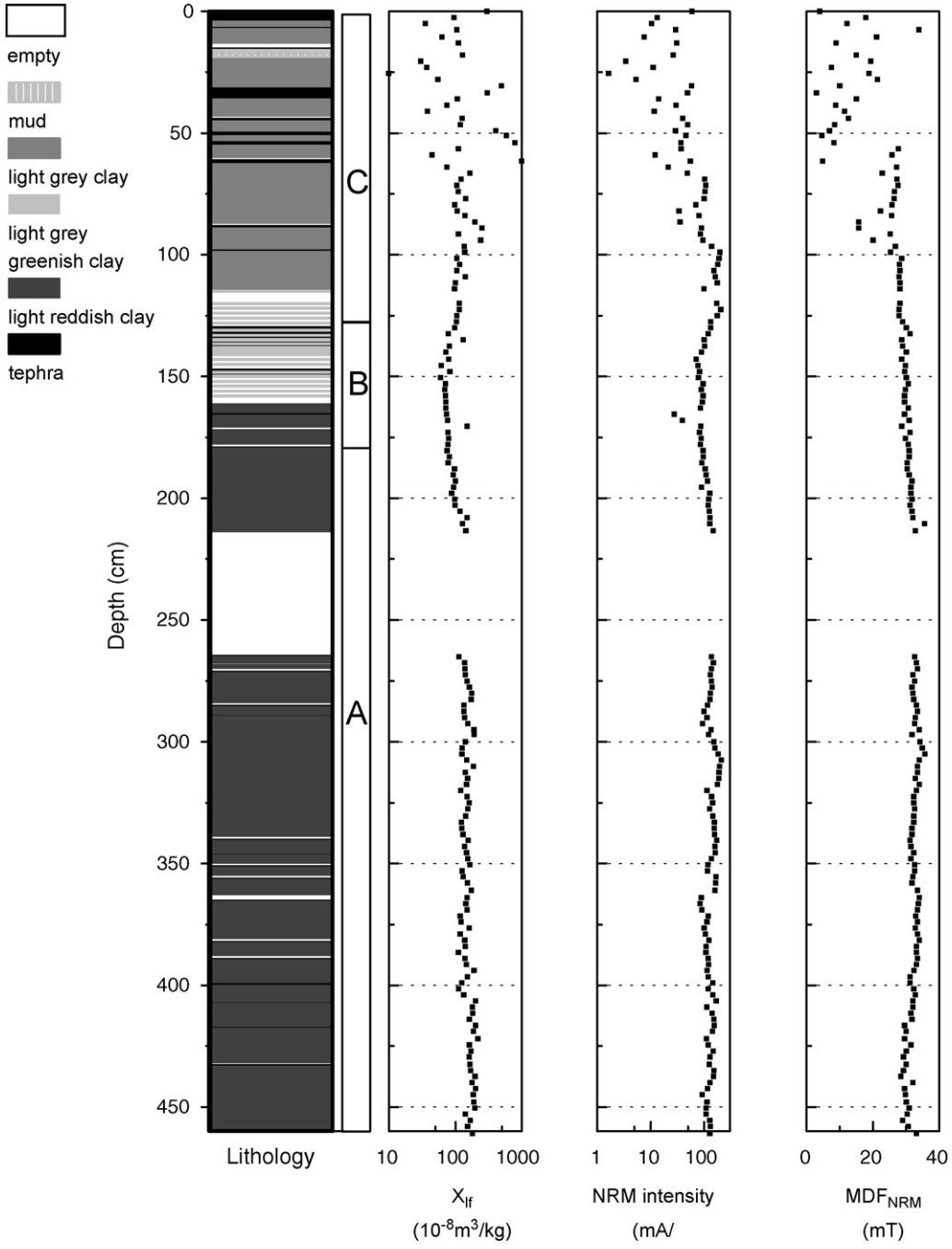

Fig. 2. Logs of lithology, facies, specific susceptibility (X_{lf}), intensity of natural remanent magnetisation (NRM intensity) and median destructive field of the NRM (MDF_{NRM}), for core lmor-1 vs. depth.

suggests that NRM intensity is mainly controlled by changes in the mineral composition of the sediment and not by variations of the geomagnetic field intensity. Good consistency between X_{lf}, NRM intensity and lithology is observed in the first 100 cm. X_{lf} and NRM show higher scatter in this section than in deeper sediments and this is consistent with the more variable lithology. Lower values of susceptibility and NRM intensity generally correlate to lithologies with organic material and distinct highs in X_{lf} and NRM intensity are due to layers with volcanic ash content. The high values of X_{lf} and NRM at the top of the sequence and about 38 cm correspond with thick layers of tephra and the peaks between 50 and 63 cm (more pronounced in X_{lf} profile) correspond to several thin consecutive tephra layers. The distinct highs in X_{lf} and NRM intensity are also characterized by low coercivities.

Several studies were carried out to assess the reliability of the sediments for paleointensity investigations (Banerjee et al., 1981; King et al., 1982, 1983; Tauxe, 1993). Common requirements are that the remanence must be carried by stable magnetite grains ranging in size from 1 to 15 μm and that the variations in concentration must be less than an order of magnitude. Samples that did not meet these criteria were omitted from our estimates of relative paleointensity (30%).

The bilogarithmic plot of k vs. SIRM illustrates how the concentration and magnetic grain size of magnetite crystals in a rock can be estimated from these magnetic parameters (Thompson and Oldfield, 1986). The magnitudes of k and SIRM give the concentration, and their ratio indicates the magnetic grain size. The plot of k vs. SIRM for Lake Moreno cores shows that grain size varies between 1 and 8 μm and concentration varies between 0.02 and 0.2% (Fig. 3(a)).

The ratios of coercivity of remanence to coercivity (H_{CR}/H_C) and saturation remanence to saturation magnetisation (M_{RS}/M_S) are sensitive to variations in grain size (Day et al., 1977; Dunlop, 1986). The hysteresis parameter ratios, H_{CR}/H_C and M_{RS}/M_S, vary between 2.5 and 3.8, and 0.14 and 0.25, respectively (Fig. 3(b)) and typical coercivity (H_C) values range from 10.9 to 24 mT. These results suggest that pseudo-single domain (PSD) magnetite or titanomagnetite is the dominant magnetic mineral in the samples. Hysteresis loops indicate saturation fields well below 400 mT, typical coercivities for magnetite (Richter et al., 2006).

IRM acquisition curves in fields up to 1.2 T indicate that about 90% of the SIRM is obtained between 200 and 300 mT (Fig. 3(c)). Thermal demagnetisation experiments were carried out on 30 samples from the sediment core. Some representative stepwise thermal demagnetisation curves of SIRM are displayed in Fig. 3(d). In general, two main magnetic phases and eventually a third one were observed. Each phase is mainly discriminated from slope changes in the curve of remanent magnetisation; hence T_Us were determined.

The unblocking temperatures of the first phases vary slightly between 150 °C and about 250 °C, as can be noted in samples 18, 32, 99 and 124. Slope changes are particularly notorious in samples from the upper section (e.g., 18, 32). These changes at low temperature were also observed by Dankers (1978) in titanomagnetite (titanomaghemite, maghemitised exsolved titanomagnetite) and maghemite specimens. Other samples, like 99 and 124, show a linear decrease without important changes in the RM curve; however, this behaviour may also be due to titanomagnetite.

The unblocking temperatures of the second component vary between 530 °C (samples 18, 32, 99) and 580 °C (124, 153); and the RM decreases mostly linearly for all samples. The most important changes in RM are observed in this second magnetic phase; note that about 80% of the RM is lost in these steps, so it can be considered the main magnetic phase. These T_Us are interpreted as Ti-poor titanomagnetite and magnetite minerals, respectively (Dankers, 1978; Hunt et al., 1995; Dunlop and Özdemir, 1997).

Since the RMs do not completely vanish at temperatures above the Curie temperature of magnetite (580 °C), the presence of hard magnetic minerals is expected. The temperatures of this third non-

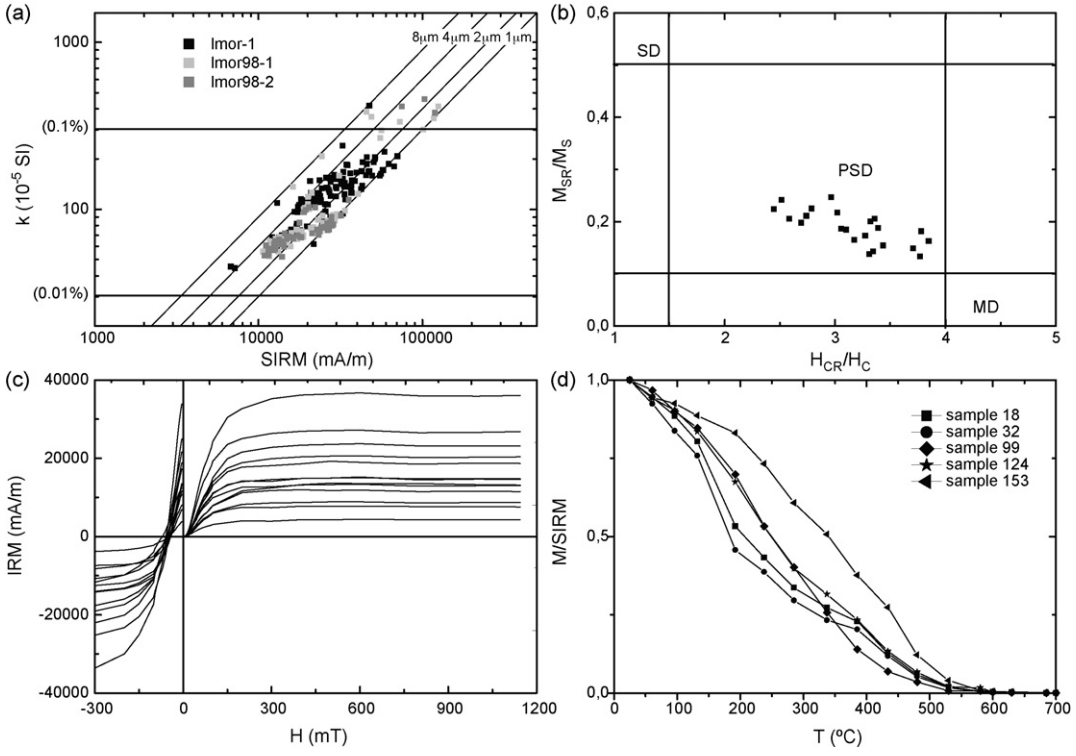

Fig. 3. (a) k vs. SIRM for all samples in order to estimate concentration and grain size according to Thompson and Oldfield (1986). (b) Hysteresis parameter ratios, H_{CR}/H_C vs. M_{RS}/M_S for estimation of grain size. (c) IRM acquisition curves of samples from different lithologies. (d) Thermal demagnetisation curves of SIRM for five samples.

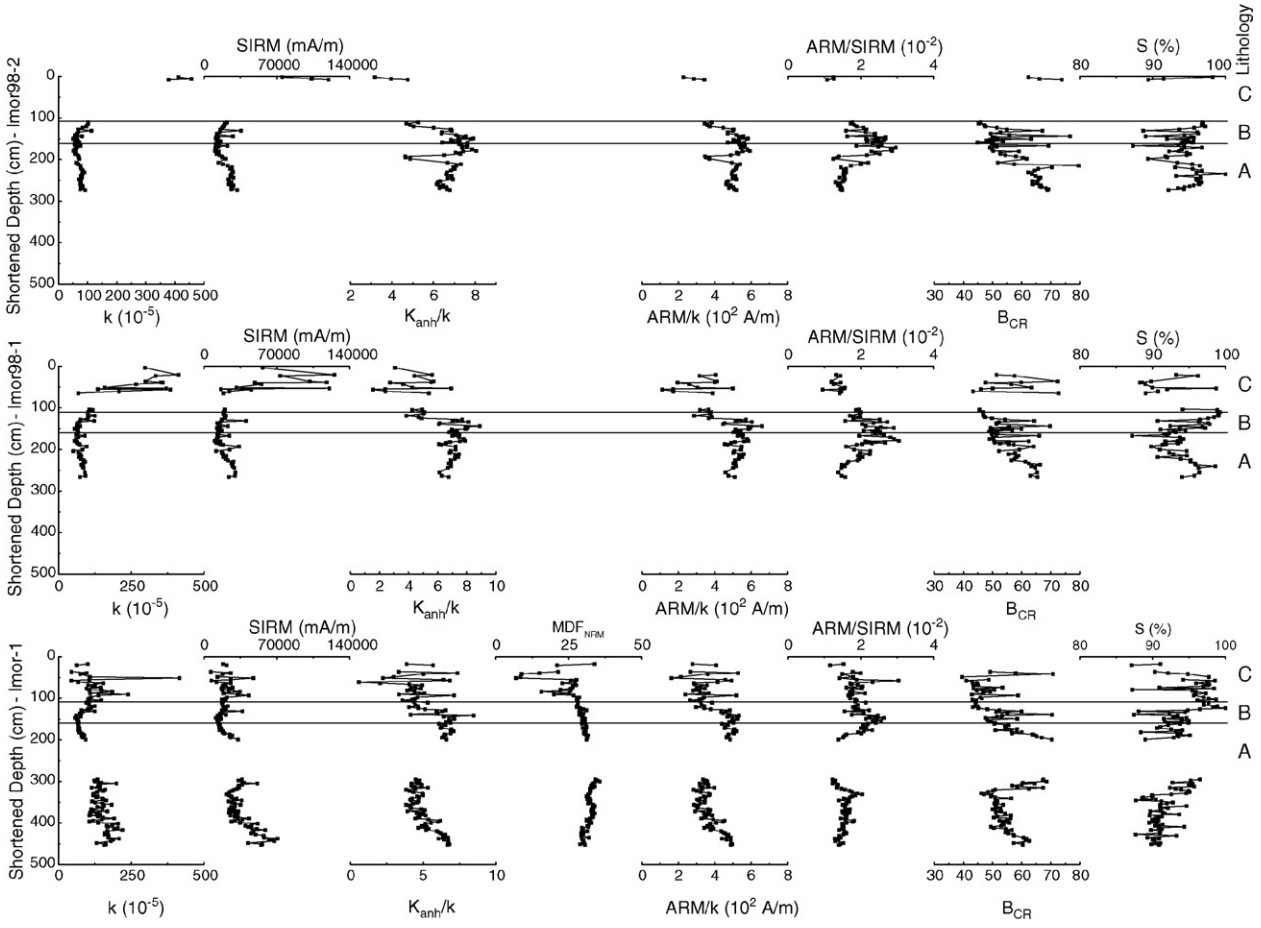

Fig. 4. Down-core variation of selected rock magnetic properties for the lmor-1, lmor98-1 and lmor98-2 cores.

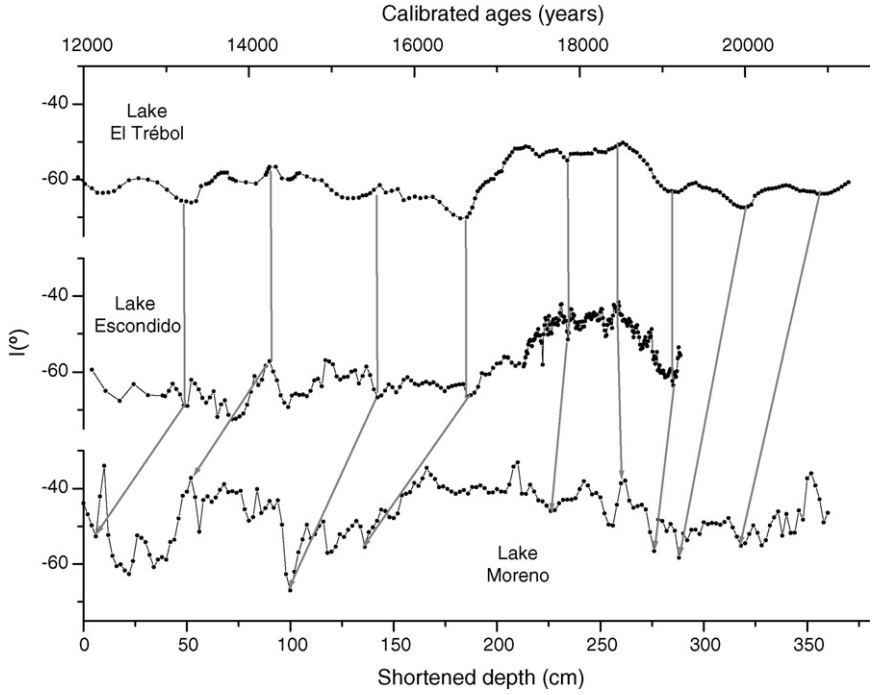

Fig. 5. Paleomagnetic dating of Lake Moreno sediments. The master dated curves are from Lake Escondido (Gogorza et al., 2002) and Lake El Trébol (Irurzun et al., 2006). Some correlation tie lines are shown.

significant phase vary between 600 and 685 °C and correspond to maghemite and hematite. However, these results should be considered with care because of the low RM and the possibility of neo-formation of the magnetic minerals as suggested from the magnetic susceptibility changes.

Fig. 4 shows down-core logs of several magnetic parameters and ratios between them. The variation in the concentration of magnetic carriers was investigated by using the concentration dependence of SIRM and k. The range of values for k and SIRM intensities through the stratigraphic sequences ($45–240 \times 10^{-5}$ SI except for a peak value of k of about 415×10^{-5} SI, and 10–100 A/m, except for three samples that exhibit SIRM values of about 120 A/m) indicates variations of the same order of magnitude. As in our previous studies (Gogorza et al., 2004, 2006), the more pronounced variations in concentration were observed in the upper 100 cm, corresponding to lithology C ("Lake Moreno" facies). On the other hand, an increase in concentration down-hole was suggested by the increasing trend observed in SIRM and k in lithology A.

Magnetic grain size can be also estimated from the concentration-independent inter-parametric ratios k_{ARM}/k, ARM/k and ARM/SIRM (Fig. 4). Like the changes in concentration, variations in magnetic grain size are more substantial in lithology C than in lithologies A and B. The k_{ARM}/k ratio can be used to estimate relative variations in magnetic grain size if the magnetisation is dominated by magnetite (Richter et al., 2006). The k_{ARM}/k ratio (Fig. 4) shows erratic behaviour in lithology C, which suggests sharp variations in magnetite grain size. Close to the position of the boundary between lithologies C and B, a steep increase in the k_{ARM}/k ratio from about 5 (below 115 cm) to 7.5 (above 115 cm) is present, suggesting a decrease in grain size. Between 115 cm and 270 cm, the ratio remains close to this value, while below this depth it drops to about 4, suggesting coarser grain size; from 350 cm to the bottom of the core there is a sustained increase in the ratio in lmor-1, suggesting a decreasing grain size. This last increase could not be observed in the other cores because there are few or no samples for this section. Similar behaviour is observed in ratios ARM/k and ARM/SIRM, but with a different pattern in the last between 400 and 450 cm (Fig. 4). In this last section, we observe an increase in the k_{ARM}/k ratio and a decrease in the ARM/SIRM ratio. k_{ARM}/k ratio and ARM/SIRM ratio are the proxies generally used to estimate grain size. The latter concerns only remanent magnetisations and is thus independent of paramagnetic and diamagnetic components.

Variations in the coercivities of magnetic minerals were investigated with the median destructive field of the NRM (MDF_{NRM}) and median destructive field of the ARM (MDF_{ARM}). Down-core

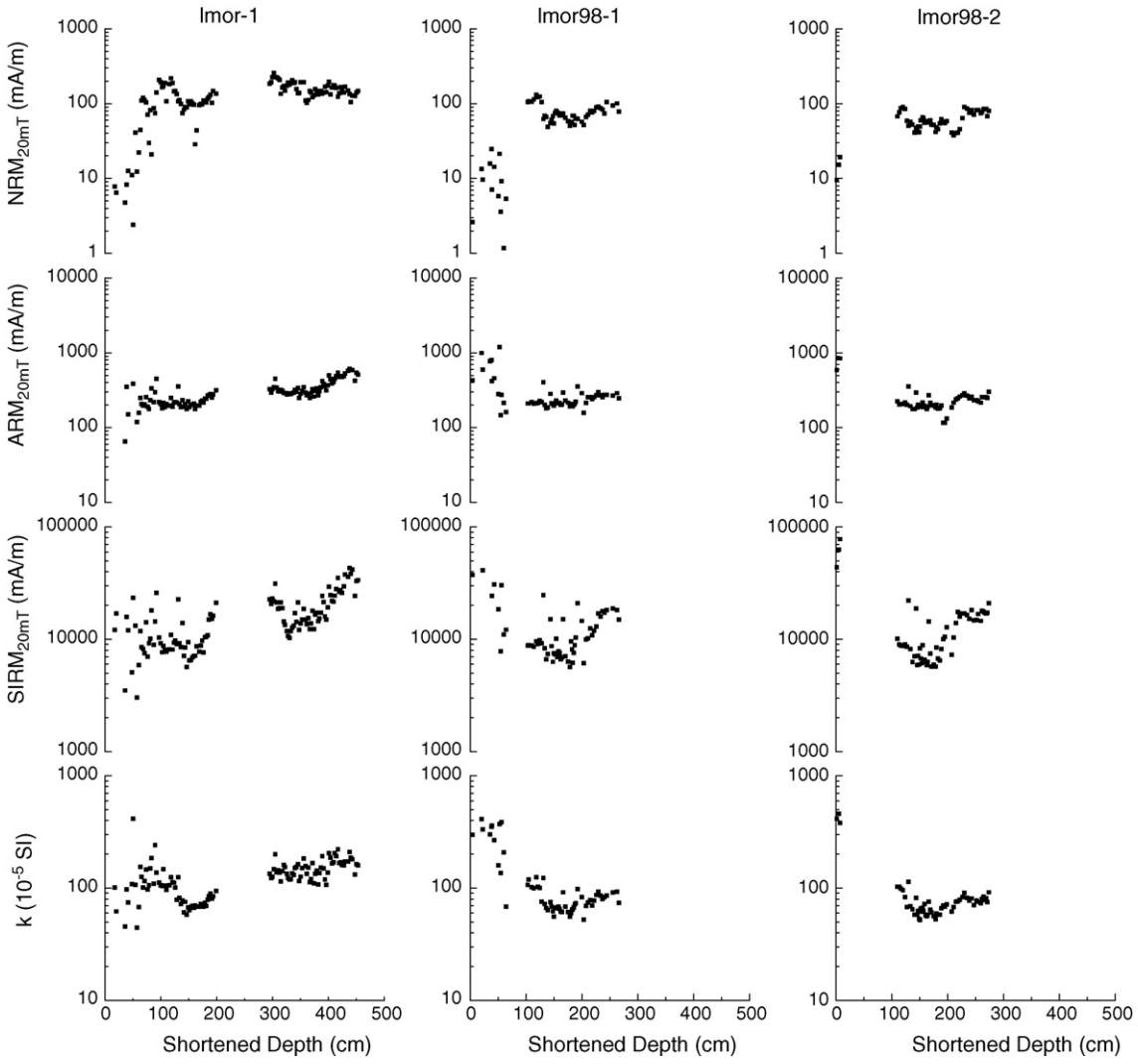

Fig. 6. k, $SIRM_{20mT}$, ARM_{20mT} and NRM_{20mT} records vs. shortened depth from cores lmor-1, lmor98-1 and lmor98-2.

variations of MDF_{NRM} are very small (28–36 mT) between 115 and 300 cm (lithologies A and B), reflecting a homogeneous distribution of the magnetic minerals. In the upper part (0–115 cm, lithology C), MDF_{NRM} changes significantly and reaches minimum values (8 mT) at 50 and 80 cm, which may be due to an increase in low-coercivity minerals and/or the magnetic grain size. MDF_{ARM} varies in the narrow range of 22–27 mT along the core, except for a few horizons, proving that the ARM was only acquired by the low-coercivity fraction, identified with magnetite (Sagnotti et al., 2001). The B_{cr} pattern along the cores is very similar to the ARM/k pattern, which is consistent with the changes in grain size described above. Measurements of the S_{ratio} ($-IRM_{-300\,mT}$/SIRM) (Bloemendal et al., 1992) vary between 0.87 and 1, illustrating the dominance of low-coercivity magnetic minerals. The generally high values indicate that magnetite is probably the most abundant magnetic mineral in the cores. These rock magnetic results indicate that the magnetic signal in the clay-rich sediments is dominated by (low-titanium) magnetite and that the sediments fulfil the criteria required for paleointensity studies.

5. Chronology

In order to date the RPI records, we chose a time–depth function obtained from PSV correlation to nearby lakes (Fig. 5), rather than a model based on radiocarbon dates. The chronology was therefore defined by previous results: distinctive magnetic features of declination and inclination of Lake Moreno were identified and correlated with similar features in Lake El Trébol and Lake Escondido sediments, which were dated using AMS (Gogorza et al., 2002; Irurzun et al., 2006). The proximity of the sample sites (about 5 km) guarantees that the inclination and declination features in the cores are synchronous (Irurzun et al., 2008).

6. Paleomagnetic results

6.1. Stability of intensity and direction magnetisation

Complete removal of any possible viscous component or magnetic overprint was achieved at low fields (10–15 mT) (Irurzun et al., 2008) and a characteristic remanence was clearly identified and determined with principal component analysis (Kirschvink, 1980). We have chosen the value of the NRM after the 20 mT step as representative of the stable characteristic remanent magnetisation ($NRM_{20\,mT}$) and we have used this value to construct the normalised intensity records.

6.2. Estimation of RPI by normalising methods

To obtain an estimate of RPI, NRM needs to be normalised to correct for an overall environmental signal (Tauxe, 1993). Although a consensus on a preferred normaliser has not been reached, it appears that we can make use of any normaliser if the sediment is magnetically homogeneous and the characteristic component of magnetisation has been isolated (Valet and Meynadier, 1998). Johnson et al. (1975) and Levi and Banerjee (1976) proposed to use the remanence whose "demagnetisation curve most closely resembles that of the NRM". According to Valet (2003), the ARM is preferred, because this parameter offers the advantage of dealing with single- or PSD magnetite grains. Moreover, Levi and Banerjee (1976) affirmed that NRM and ARM demagnetisation curves should

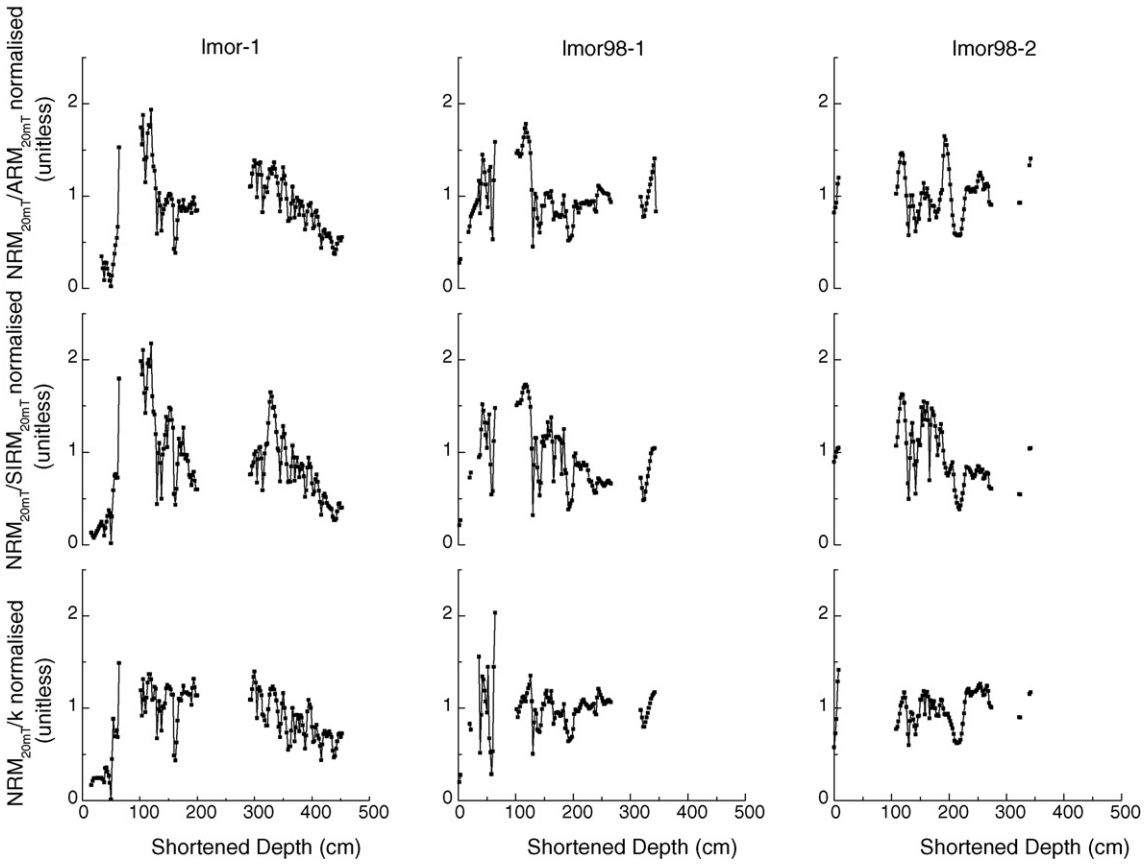

Fig. 7. Normalised $NRM_{20\,mT}/k$, $NRM_{20\,mT}/SIRM_{20\,mT}$ and $NRM_{20\,mT}/ARM_{20\,mT}$ records vs. shortened depth from cores lmor-1, lmor98-1 and lmor98-2.

be similar to determine the common range of coercivities (and/or blocking temperatures) involved in both magnetisations.

The seemingly most reasonable normalisers are ARM and IRM, which are remanence based, and often resemble the NRM in their demagnetisation behaviour. We also use magnetic susceptibility, but its signal encompasses paramagnetic and large multi-domains grains, which contribute little or nothing to NRM (Hofmann and Fabian, 2007).

In general, NRM, ARM and SIRM are used after AF demagnetisation at 20 mT. This AF peak field is enough to remove the secondary components present in the NRM (Irurzun et al., 2008). The records of $NRM_{20\,mT}$, $ARM_{20\,mT}$, $SIRM_{20\,mT}$ and k are shown in Fig. 6 on a common depth scale for the three cores. For each core, we obtained three estimates of normalised field intensity using $ARM_{20\,mT}$, $SIRM_{20\,mT}$ and k as normalising parameters. The results are shown in Fig. 7 on a common depth-scale for all cores. There are differences in the ranges of changes in the upper ("Lake Moreno" facies) and lower ("Lake Elpalafquen" facies) sections; for this reason, the records are scaled by their respective mean values.

By comparing the relative paleointensity records obtained from the three different normalisation parameters, it turned out that while $NRM_{20\,mT}/ARM_{20\,mT}$ and $NRM_{20\,mT}/SIRM_{20\,mT}$ lead to very similar results, both deviate slightly from $NRM_{20\,mT}/k$. Due to the closer resemblance between NRM and ARM demagnetisation curves compared to IRM curves, we consider $ARM_{20\,mT}$ as the most appropriate normalising parameter (Fig. 8).

In order to get a composite profile, we stacked the individual normalised paleointensity records. We needed data at the same depth for each core, so we interpolated to get data every 2 cm. The stacking was carried out using the arithmetic mean at each interpolated sampling point and the 2σ error bars were calculated.

In order to analyze the different parameters as functions of time and to compare our results with previously published paleomagnetic records, we defined a transfer function from shortened depth to calibrated ages using the chronology explained in Section 5. Relative paleointensity profiles are shown as a function of calibrated ages in Fig. 9.

The three conventional normalisation methods yield profiles with broad similarities but differ in the amplitudes of peaks and troughs. The $NRM_{20\,mT}/k$ ratio shows lower amplitudes between

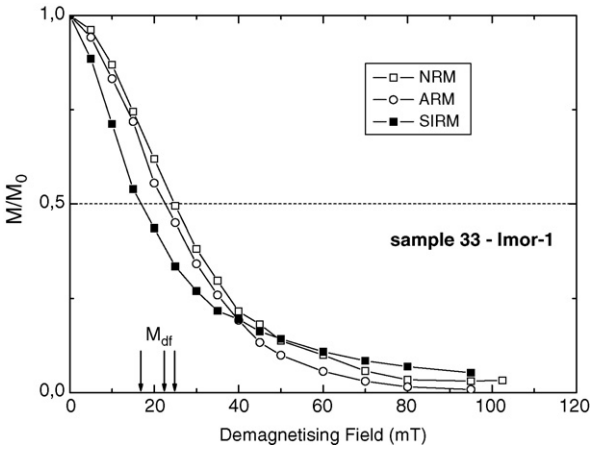

Fig. 8. Typical AF demagnetisation curves of NRM, ARM and SIRM for sample 33 (lmor-1).

14.3 and 15.9 kyr BP calibrated ages, perhaps due to the paramagnetic contribution that is reflected by k but not by ARM and SIRM. The $NRM_{20\,mT}/SIRM_{20\,mT}$ ratio shows higher amplitudes between 16.5 and 17.4 kyr BP calibrated ages, suggesting an increase in the proportion of finer grains. This is consistent with the conclusions obtained in Section 4 about a decrease in grain size close to the boundary between lithologies C and B.

6.3. Estimation of RPI by a pseudo-Thellier method

In general, the pseudo-Thellier approach successfully estimates relative paleointensities from sedimentary cores (Tauxe, 1993; Kok, 1998; Kruiver et al., 1999; Brachfeld and Banerjee, 2000; Pan et al., 2001; Snowball and Sandgren, 2004). In some cases, like studies on sediments from the Ongtong-Java Plateau (Tauxe et al., 1995) the pseudo-Thellier method provides considerably different results from the conventional normalisation method.

In this paper, we determine paleointensities by the pseudo-Thellier method, following Tauxe et al. (1995) using ARM on 65 samples of lmor-1 core. According to Tauxe et al. (1995), we use

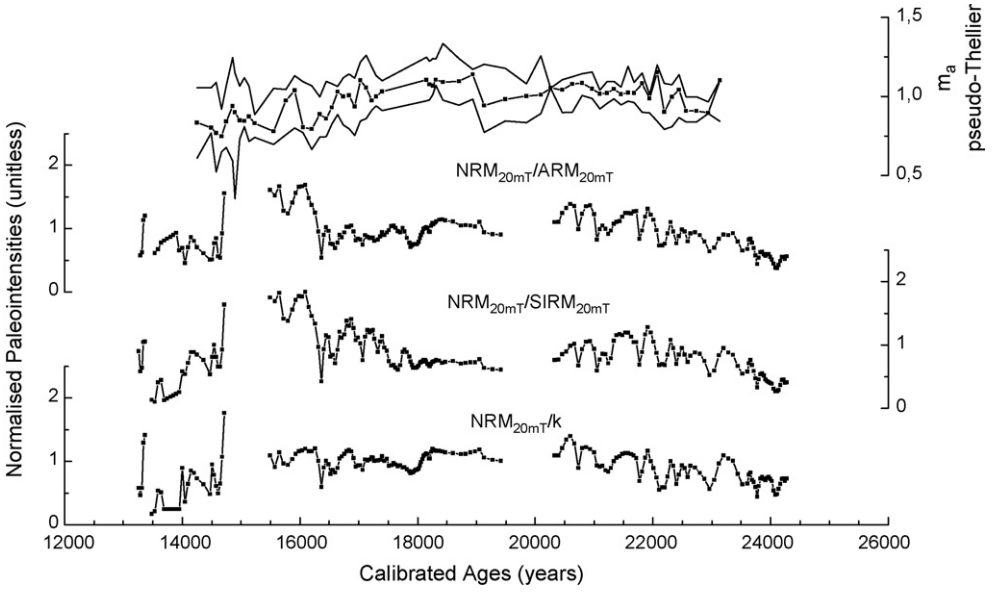

Fig. 9. m_a (pseudo-Thellier method) and stacked $NRM_{20\,mT}/ARM_{20\,mT}$, $NRM_{20\,mT}/SIRM_{20\,mT}$ and $NRM_{20\,mT}/k$ records vs. calibrated ages.

ARM and not IRM acquisition because it was showed that the plot of ARM left vs. ARM gained at the same peak field is somewhat linear, whereas IRM left vs. IRM gained is markedly curved. The estimation procedure combines Jackknife resampling with robust regression, an alternative version of the methods followed by Kok (1998) and Kruiver et al. (1999) that has proved to produce better estimation results (Gogorza et al., in press).

Initially, the Jackknife method was used to determine several regression slope estimates (sub-samples) in every sample, considering all, all but one, all but two and all but three field values (whenever possible) between 30 and 60 mT (a minimum of three points in each sub-sample was required by the slope formulae). Then, robust-regression slope estimates were obtained for each of these sub-samples by using Theil's complete method (Glaister, 2005). The optimal slope (m_a) corresponding to the whole sample was finally chosen among all obtained ones as the slope producing the regression line with least sum of absolute deviations between observed and fitted values. In addition, descriptive measures of estimation goodness were calculated:

(i) The percentage of $NRM_{20\,mT}/ARM_{20\,mT}$ lmor-1, $NRM_{20\,mT}/ARM_{20\,mT}$ lmor98-1 and $NRM_{20\,mT}/ARM_{20\,mT}$ lmor98-2 reference values lying inside the D1–D9 band (Kok et al., 1998), being 23.03, 36.36 and 51.14%, respectively, with a global value of 33.96%.

(ii) The average of these three reference values was also calculated; it was trapped in the band in 33.04% of cases. The RPI results obtained by the pseudo-Thellier method (m_a) for 65 specimens are plotted in Fig. 9 for comparison with the values obtained by normalising using $ARM_{20\,mT}$, $SIRM_{20\,mT}$ and k.

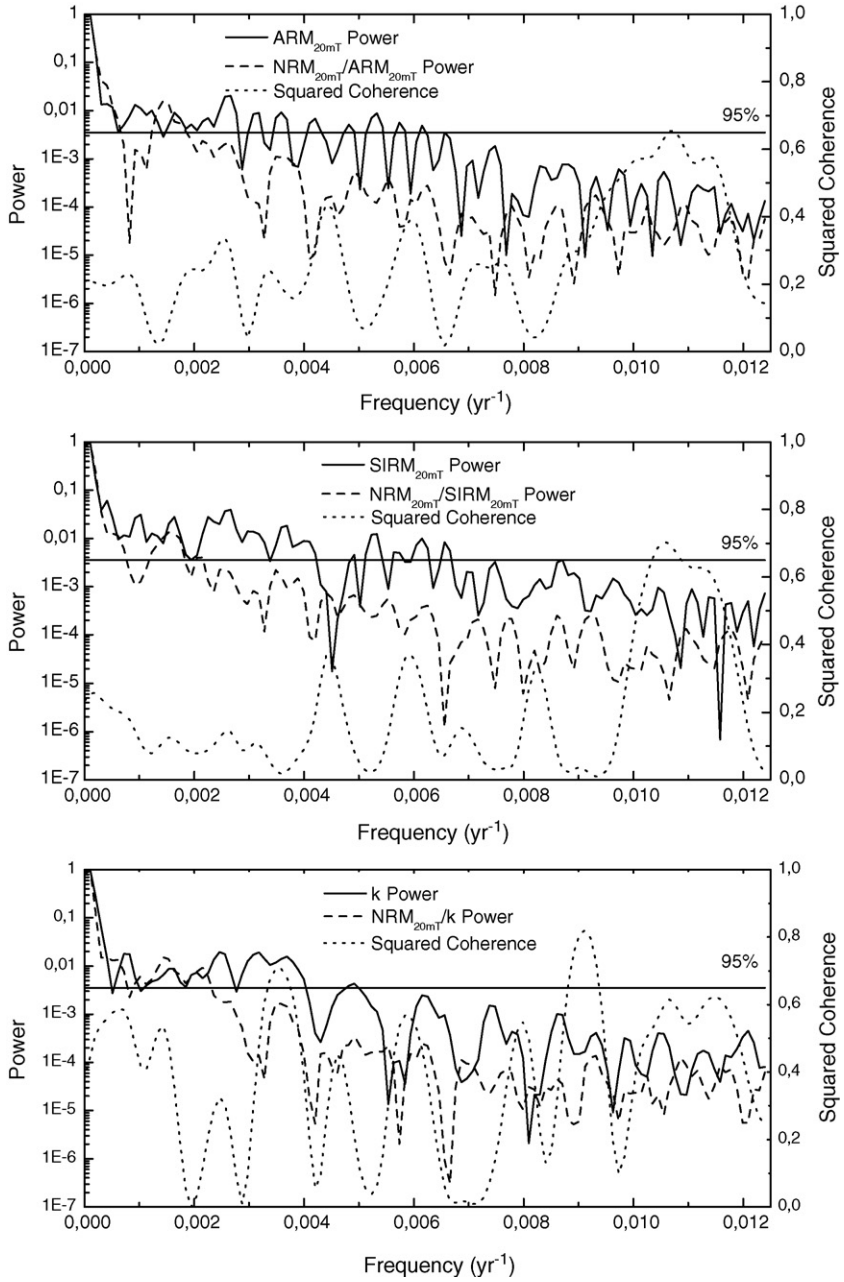

Fig. 10. Spectral analysis of three normalisation parameters ($ARM_{20\,mT}$, $SIRM_{20\,mT}$ and k) and three normalised remanences ($NRM_{20\,mT}/ARM_{20\,mT}$, $NRM_{20\,mT}/SIRM_{20\,mT}$ and $NRM_{20\,mT}/k$). Coherence tests results are shown. The 95% confidence level is denoted by the horizontal line.

There are enough similarities between the pseudo-Thellier data and the normalised profiles, which is not surprising for young sediments unaffected by viscous overprint. The peaks at about 14 and 15.9 kyr BP calibrated ages recorded by conventional methods are also observed in pseudo-Thellier record, although they are not so pronounced. The behaviour between 14 and 15.5 kyr BP calibrated ages cannot be compared because there is no record for this period in the normalised profiles. The decreasing trend from 21.5 kyr BP calibrated ages to the bottom, observed in normalised records, are also present in the pseudo-Thellier data. The pseudo-Thellier data between 16.1 and 17.4 kyr BP calibrated ages are more similar to the $NRM_{20\,mT}/ARM_{20\,mT}$ and $NRM_{20\,mT}/k$ ratios than to $NRM_{20\,mT}/SIRM_{20\,mT}$.

6.4. Coherence function analysis

We used MATLAB 6.1 software to detect the presence of harmonic components in the data series. We first examined the power spectra for ARM, SIRM and k and the normalised records ($NRM_{20\,mT}/ARM_{20\,mT}$, $NRM_{20\,mT}/SIRM_{20\,mT}$ and $NRM_{20\,mT}/k$) and then carried out a coherence function analysis on the records to test the efficiency of the normalisations in removing the effects of climatic/environmental factors over specific frequency ranges (Fig. 10). If the paleointensity record ($NRM_{20\,mT}/ARM_{20\,mT}$, etc.) and the related normaliser ($ARM_{20\,mT}$, etc.) do not show significant coherence, one can have confidence that the paleointensity normalisation is not significantly affected by lithological or other environmental factors.

The analyses suggest that the normalised curves are not coherent with the parameters of normalisation and that the records are not affected by climatic or lithologic factors, but represent a true geomagnetic signal. The best results are obtained for $ARM_{20\,mT}$ because at 95% confidence level no coherence is found. These results are consistent with the results suggested by grain size and concentration analysis. The spectral analysis of normalised remanences, normalisation parameters and coherence test were carried out following the method of Tauxe and Wu (1990).

7. Comparison with other records

In order to assess the validity of the paleointensity records, we compared them with paleointensity stacks reconstructed for Southern Hemisphere (Fig. 11(a) and (b)). In Fig. 11(a) the comparison is restricted to records with radiocarbon chronologies: our records –the previous results from Lake Escondido (Gogorza et al., 2004) and Lake El Trébol (Gogorza et al., 2006)—and the record of Lake Barrine (Constable, 1985) whose chronology is a hybrid ^{14}C/Calendar age. Fig. 11(b) shows our present record, the results from South Atlantic geomagnetic paleointensity stack, SAPIS (Stoner et al., 2002) and one of the three cores (SEDANO) collected from Antarctic late Pleistocene sediments (Sagnotti et al., 2001). In these cases, relative paleointensities are represented against calibrated ages.

7.1. Southwestern Argentina

The comparison is restricted to the interval 11–21 ^{14}C kyr BP, which is the period of time spanned by Lake Moreno record (Fig. 11(a)). These results confirm the existence of an increase in paleointensity between 13.2 and 13.7 ^{14}C kyr BP or between 15.6 and 16.3 kyr BP calibrated age that we found in our previous work, although the higher values recorded in Lake Escondido sediments stretches more than in El Trébol and Moreno. It is important to point out that there are no distinctive changes in the concentration or grain size that account for these increases in paleointensity, which may genuinely reflect changes in the geomagnetic signal. Another characteristic that we confirmed by our Moreno results is a long decreasing trend, which was already recorded in Lake El

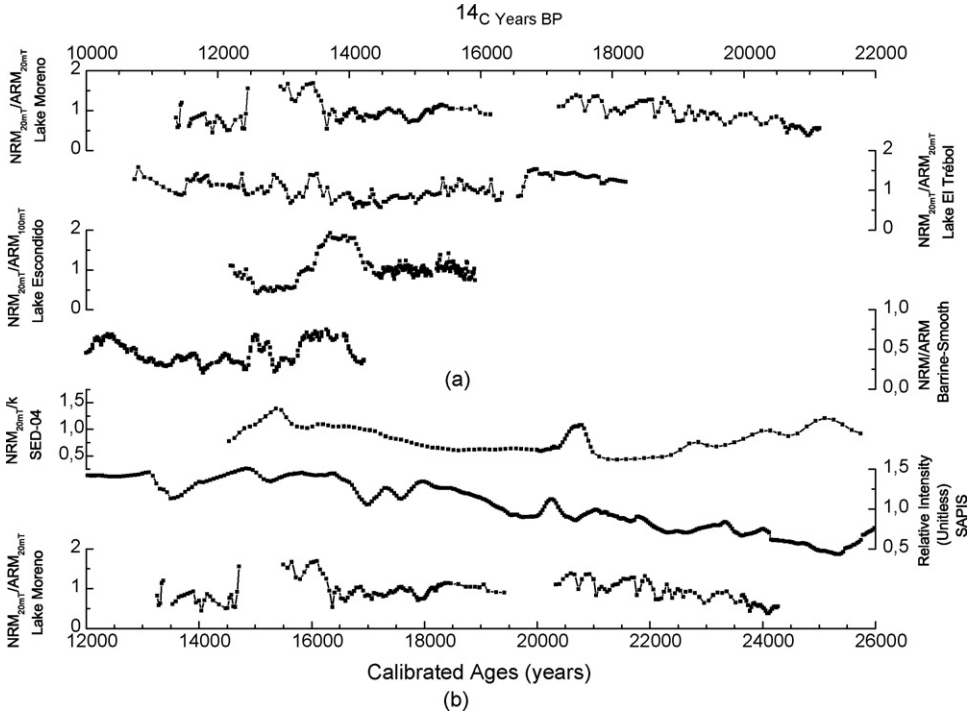

Fig. 11. (a) Comparison of normalised intensity record from the Lake Moreno stack with relative paleointensity records from Lake El Trébol and Lake Escondido in radiocarbon ages, Lake Barrine (chronology: an hybrid ^{14}C/Calendar age). (b) Comparison of normalised intensity record from the Lake Moreno stack with SED-04 core and SAPIS stack in calibrated ages.

Trébol, starting at about 16.8 ^{14}C kyr BP or 19.7 kyr BP calibrated ages (Fig. 11(a)).

7.2. Southern Hemisphere

Fig. 11(a) also shows the comparison of our records with the relative paleointensity from Lake Barrine (Australia) (Constable, 1985). The significant high observed in Lake Escondido and Moreno is also detected in Lake Barrine, although it is not exactly coincident either in time or in amplitude. The long decrease observed in Lake Moreno and Lake El Trébol is also detected in SAPIS (Fig. 11(b)). Although the SED-04 record presents much less data due to the different sedimentation rates that usually characterize the marine record, the general trend is similar. Higher values appear between 14.5 and 16 kyr BP and around 18.2 kyr BP (both in calibrated age); these features could be correlated with increases in the Lake Moreno record (Fig. 11(b)).

8. Conclusions

This paper is part of a series of papers designed to provide information about paleosecular variations and relative paleointensity records in Southern Argentina. We present here rock magnetic measurements and relative paleointensity records of three sediment cores from Lake Moreno.

The main conclusions are:

1. The composite curve of $NRM_{20\,mT}/ARM_{20\,mT}$ represents an estimate of geomagnetic paleointensity variations in southwestern Argentina for the period 13–24 kyr BP calibrated ages.
2. The dominant remanence carrier is magnetite and titanomagnetite within PSD domain grain size.
3. The down-core logs of several magnetic parameters and ratios suggest coarser grain size in the upper part of the sequence (lithology C), which becomes finer towards lithology B. The grain size seems again coarser at the beginning of lithology A.
4. The mineral concentration changes are within a factor 10, between 0.02 and 0.2%. An increase in the concentration downhole is suggested by the increasing trend observed in SIRM and k in lithology A.
5. The paleointensity records determined by conventional normalising methods and by the pseudo-Thellier method are almost consistent.
6. Many individual features of our records are observed in other regional and global paleointensity records. From a comparison of relative paleointensity records, we confirmed two significant features recorded in the sediment from SW Argentina and suggested in records from other areas of Southern Hemisphere.

Acknowledgments

The authors wish to thank Universidad Nacional del Centro de la Provincia de Buenos Aires, Instituto Antártico Argentino and Consejo Nacional de Investigaciones Científicas y Técnicas de la República Argentina (CONICET). The authors are also indebted to the anonymous reviewers for their useful suggestions for improving the manuscript.

References

Banerjee, S.K., King, J., Marvin, J., 1981. A rapid method for magnetic granulometry with applications to environmental studies. Geophys. Res. Lett. 8, 333–336.
Bianchi, M.M., Masaferro, J., Roman Ross, G., Amos, A.J., Lami, A., 1999. Late Pleistocene and Early Holocene ecological response of Lake El Trébol (Patagonia, Argentina) to environmental changes. J. Paleolimnol. 22, 137–148.
Blanchet, C.L., Touveny, N., de Garidel-Thoron, T., 2006. Evidence for multiple paleomagnetic intensity lows between 30 and 50 ka BP from a western Equatorial Pacific sedimentary sequence. Quat. Sci. Rev. 252, 162–179.
Bloemendal, J., King, J.W., Hall, F.R., Doh, S.J., 1992. Rock magnetism of Late Neogene and Pleistocene deep-sea sediments: relationship to sediment source, diagenetic processes, and sediment lithology. J. Geophys. Res. 97, 4361–4375.
Brachfeld, S.A., Banerjee, S.K., 2000. A new high-resolution geomagnetic relative paleointensity record for the North American Holocene: a comparison of sedimentary and absolute intensity data. J. Geophys. Res. 105 (B1), 821–834.
Brachfeld, S.A., Domack, E., Kisel, C., Laj, C., Leventer, A., Ishman, S., Gilbert, R., Camerlenghi, A., Eglinton, L.B., 2003. Holocene history of the Larsen-A Ice Shelf constrained by geomagnetic paleointensity dating. Geology 31 (9), 749–752.
Constable, C.G., 1985. Eastern Australian geomagnetic field intensity over the last 14000 yr. Geophys. J. Roy. Astr. Soc. 81, 121–130.
Dankers, P.H.M., 1978. Magnetic Properties of Dispersed Natural Iron-oxides of Known Grain-size. Thesis. State University of Utrecht, 142 pp.
Day, R.M., Fuller, D., Schmidt, V.A., 1977. Hysteresis properties of titanomagnetite: grain size and composition dependence. Phys. Earth Planet. Inter. 13, 260–266.
del Valle, R.A., Lirio, J.M., Nuñez, H.J., Tatur, A., Rinaldi, C.A., 2000. Sedimentary cores from Mascardi Lake, Argentina: a key site to study Elpalafquen paleolake. In: Smolka, P., Volkheimer, W. (Eds.), Southern Hemisphere Paleo and Neoclimates. Springer Verlag, Deutschland, p. 381.
Dunlop, D.J., 1986. Hysteresis properties of magnetite and their dependence on particle size: a test of pseudo-single-domain remanence models. J. Geophys. Res. 91 (B9), 9569–9584.
Dunlop, D.J., Özdemir, Ö., 1997. Rock Magnetism. Fundamentals and Frontiers. Cambridge University Press, Cambridge, 573 pp.
Glaister, P., 2005. Robust linear regression using Theil's method. J. Chem. Educ. 82, 1472–1474.
Gogorza, C.S.G., Lirio, J.M., Nuñez, H., Chaparro, M.A.E., Bertorello, H.R., Sinito, A.M., 2004. Paleointensity studies on Holocene–Pleistocene sediments from Lake Escondido, Argentina. Phys. Earth Planet. Inter. 145, 219–238.
Gogorza, C.S.G., Irurzun, M.A., Chaparro, M.A.E., Lirio, J.M., Nuñez, H., Bercoff, P.G., Sinito, A.M., 2006. Relative paleointensity of the geomagnetic field over the last 21,000 years BP from sediment cores, Lake El Trébol (Patagonia, Argentina). Earth Planet. Space 58, 1323–1332.
Gogorza, C.S.G., Sinito, A.M., Lirio, J.M., Nuñez, H., Chaparro, M.A.E., Vilas, J.F., 2002. Paleosecular variations 0–19,000 years recorded by sediments from Escondido Lake (Argentina). Phys. Earth Planet. Inter. 133, 35–55.
Gogorza, C.S.G., Sinito, A.M., Di Tomasso, I., Vilas, J.F., Creer, K.M., Nuñez, H., 1999. Holocene secular variation recorded by sediments from Lake Escondido (South Argentina). Earth Planet. Space 51, 93–106.
Gogorza, C.S.G., Torcida, S., Irurzun, M.A., Chaparro, M.A.E., Sinito, A.M., in press. A pseudo-Thellier relative paleointensity record during the last 18,000 years from Lake El Trébol (Patagonia, Argentina). Geofísica Internacional.
Guyodo, Y., Valet, J.P., 1996. Relative variations in geomagnetic from sedimentary records: the past 200,000 years. Earth Planet. Sci. Lett. 143, 23–36.
Hofmann, D.I., Fabian, K., 2007. Rock magnetic properties and relative paleointensity stack for the last 300 ka based on a stratigraphic network from the subtropical and subantarctic South Atlantic. Earth Planet. Sci. Lett. 260, 297–312.
Hunt, C.P., Banerjee, S.K., Han, J., Solheid, P.A., Oches, E., Sun, W., Liu, T., 1995. Rock-magnetic proxies of climate change in the loess-paleosol sequences of the western Loess Plateau of China. Geophys. J. Int. 123, 232–244.
Irurzun, M.A., Gogorza, C.S.G., Sinito, A.M., Lirio, J.M., Nuñez, H., Chaparro, M.A.E., 2006. Paleosecular variations recorded by sediments from Lake El Trébol, Argentina. Phys. Earth Planet. Inter. 154, 1–17.
Irurzun, M.A., Gogorza, C.S.G., Sinito, A.M., Chaparro, M.A.E., Nuñez, H., Lirio, J.M., 2008. Paleosecular variations 12–20 kyr as recorded by sediments from Lake Moreno (Southern Argentina). Stud. Geophys. Geod. 52 (2), 157–172.
Johnson, H.P., Kinoshita, H., Merrill, R.T., 1975. Rock magnetism and paleomagnetism of some North Pacific deep-sea sediments. Geol. Soc. Am. Bull. 86, 412–420.
King, J., Banerjee, S.K., Marvin, J., Özdemir, Ö., 1982. A comparison of different magnetic methods for determining the relative grain size of magnetite in natural materials: some results from lake sediments. Earth Planet. Sci. Lett. 59, 404–419.
King, J.W., Banerjee, S.K., Marvin, J., 1983. A new rock magnetic approach to selecting sediments for geomagnetic paleointensity studies: application to paleointensity for the last 4000 years. J. Geophys. Res. 88, 5911–5921.
Kirschvink, J.L., 1980. The least-square line and plane and the analysis of paleomagnetic data. Geophys. J. R. Astron. Soc. 62, 699–718.
Kok, Y.S., 1998. Relative Paleointensities of the Earth's Magnetic Field Derived From Deep-sea Sediments. Reading The Muddy Compass (PhD Thesis Utrecht University). Geologica Ultraiectina, 165, 131 pp.
Kruiver, P.P., Kok, Y.S., Dekkers, M.J., Langereis, C.G., Laj, C., 1999. A pseudo-Thellier relative paleointensity record, and rock magnetic and geochemical parameters in relation to climate during the last 276 kyr in the Azores region. Geophys. J. Int. 136, 757–770.
Levi, S., Banerjee, S.K., 1976. On the possibility of obtaining relative paleointensities from lake sediments. Earth Planet. Sci. Lett. 29, 219–226.
Macri, P., Sagnotti, L., Lucchi, R.J., Rebesco, M., 2006. A stacked record of relative geomagnetic paleointensity for the past 270 kyr from the western continental rise of the Antarctic Peninsula. Earth Planet. Sci. Lett. 252, 162–179.
Pan, Y., Zhu, R., Shaw, J., Liu, Q., Guo, B., 2001. Can relative paleointensities be determined from the normalised magnetisation of the wind-blown loess of China? J. Geophys. Res. 106 (B9), 19221–19232.

Peck, J.A., King, J.W., Colman, S.M., Kravchinsky, V.A., 1996. An 84-kyr paleomagnetic record from the sediments of Lake Baikal, Siberia. J. Geophys. Res. 101 (B5), 11365–11385.

Richter, C., Venuti, A., Verosub, K.L., Wei, K., 2006. Variations of the geomagnetic field during the Holocene: relative paleointensity and inclination record from the West Pacific (ODP Hole 1202B). Phys. Earth Planet. Inter. 156, 179–193.

Sagnotti, L., Macri, P., Camerlenghi, A., Rebesco, M., 2001. Environmental magnetism of Antarctic Late Pleistocene sediments and interhemispheric correlation of climatic events. Earth Planet. Sci. Lett. 192, 65–80.

Stoner, J.S., Laj, C., Channell, J.E.T., Kissel, C., 2002. South Atlantic and North Atlantic geomagnetic paleointensity stacks (0–80 ka): implications for interhemispheric correlation. Quat. Sci. Rev. 21, 1141–1151.

Snowball, I., Sandgren, P., 2004. Geomagnetic field intensity changes in Sweden between 9000 and 450 cal BP: extending the record of "archaeomagnetic jerks" by means of lake sediments and the pseudo-Thellier technique. Earth Planet. Sci. Lett. 227, 361–376.

St-Onge, G., Stoner, J.S., Hillaire-Marcel, C., 2003. Holocene paleomagnetic records from St. Lawrence Estuary, eastern Canada: centennial- to millennial-scale geomagnetic modulation of cosmogenic isotopes. Earth Planet. Sci. Lett. 209, 113–130.

Tauxe, L., 1993. Sedimentary records of relative paleointensities of the geomagnetic field: theory and practice. Rev. Geophys. 31, 319–354.

Tauxe, L., Pick, T., Kok, Y.S., 1995. Relative paleointensity in sediments; a pseudo-Thellier approach. Geophys. Res. Lett. 22, 2885–2888.

Tauxe, L., Wu, G., 1990. Normalised remanence in sediments of the western Equatorial Pacific: relatively intensity of the geomagnetic field? J. Geophys. Res. 95, 12337–12350.

Thompson, R., Oldfield, F., 1986. Environmental Magnetism. Allen & Unwin Ltd, 225 pp.

Valet, J.P., 2003. Time variations in geomagnetic intensity. Rev. Geophys. 41 (1), 1004.

Valet, J., Meynadier, L., 1998. A comparison of different techniques for relative paleointensity. Geophys. Res. Lett. 25, 89–92.